Article

Templation of the Excited-State Chemistry of □-(*n*-Alkyl) Dibenzyl Ketones: How Guest Packing within a Nanoscale Supramolecular Capsule Influences Photochemistry

Corinne L. D. Gibb, Arun Kumar Sundaresan, V. Ramamurthy, and Bruce C. Gibb

J. Am. Chem. Soc., **2008**, 130 (12), 4069-4080 • DOI: 10.1021/ja7107917

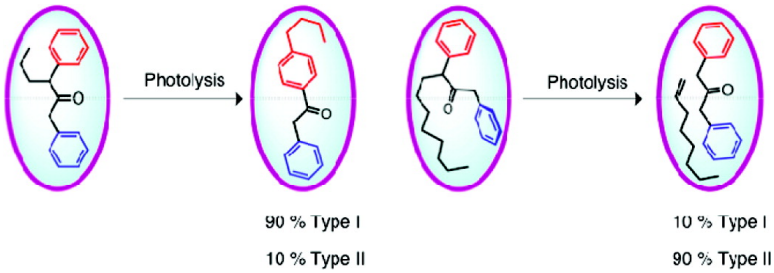

More About This Article

Additional resources and features associated with this article are available within the HTML version:

- Supporting Information
- Links to the 3 articles that cite this article, as of the time of this article download
- Access to high resolution figures
- Links to articles and content related to this article
- Copyright permission to reproduce figures and/or text from this article

View the Full Text HTML

J|A|C|S
ARTICLES
Published on Web 03/06/2008

Templation of the Excited-State Chemistry of α-(*n*-Alkyl) Dibenzyl Ketones: How Guest Packing within a Nanoscale Supramolecular Capsule Influences Photochemistry

Corinne L. D. Gibb,[‡] Arun Kumar Sundaresan,[†] V. Ramamurthy,*[,†] and Bruce C. Gibb*[,‡]

Department of Chemistry, University of Miami, Coral Gables, Florida 33124, and Department of Chemistry, University of New Orleans, New Orleans, Louisiana 70148

Received December 3, 2007; E-mail: murthy1@miami.edu

Abstract: Excited-state behavior of eight α-alkyl dibenzyl ketones (alkyl = CH_3 through *n*-C_8H_{17}) that are capable of undergoing type II and/or type I photoreactions has been explored in isotropic solution and within a water-soluble capsule. The study consisted of two parts: photochemistry that explored the excited-state chemistry and an NMR analysis that revealed the packing of each guest within the capsule. The NMR data (COSY, NOESY, and TOCSY experiments) revealed that ternary complexes between α-alkyl dibenzyl ketones and the capsule formed by two cavitands are kinetically stable, and the guests fall into three packing motifs modulated by the length of the α-alkyl chain. In essence, the host is acting as an external template to promote the formation of distinct guest conformers. The major products from all eight guests upon irradiation either in hexane or in buffer solution resulted from the well-known Norrish type I reaction. However, within the capsule the excited-state chemistry of the eight ketones was dependent on the alkyl chain length. The first group consisted of α-hexyl, α-heptyl, and α-octyl dibenzyl ketones that yielded large amounts of Norrish type II products within the host, while in solution the major products were from Norrish type I reaction. The second group consists of α-butyl and α-pentyl dibenzyl ketones that yield equimolar amounts of two rearranged starting ketones within the capsule (combined yield of ca 60%), while in solution no such products were formed. The third group consisted of α-methyl, α-ethyl, and α-propyl dibenzyl ketones that within the capsule yielded only one (not two) rearranged starting ketone in larger amounts (21−35%) while in solution no rearrangement product was obtained. Variation in the photochemistry of the guest within the capsule, with respect to the α-alkyl chain length of the guest, highlights the importance of how a small variation in supramolecular structure can influence the selectivity within a confined nanoscale reactor.

Introduction

The remark that Hammett made almost seven decades ago, that "a major part of the job of the chemist is the prediction and control of the course of reactions", still remains true although the techniques employed to "predict and control" reactions have changed.[1] In recent times, the use of confined media to control photoreactions has gained importance,[2−4] and we present results of one such investigation where a water-soluble, deep cavity cavitand is used as a reaction vessel.[5] In the presence of a suitable guest (or guests), two molecules of **1** assemble in aqueous solution to form supramolecular nanocapsules.[6] These capsular complexes, in which the templating guest or guests reside within an essentially dry interior, are held together by weak interactions such as van der Waals and CH−π interactions and the hydrophobic effect. Capsular assembly and disassembly are slow on the NMR time scales, and therefore in the time scale of excited-state reactions they remain essentially intact.[7]

[†] University of Miami.
[‡] University of New Orleans.

(1) (a) Hammett, L. P. *Physical Organic Chemistry, Reaction Rates, Equilibria and Mechanisms*; McGraw-Hill: New York, 1940. (b) Hammett, L. P. *Physical Organic Chemistry, Reaction Rates, Equilibria, and Mechanisms*, 2nd ed.; McGraw-Hill: New York, 1970.
(2) (a) *Photochemistry in Organized and Constrained Media*; Ramamurthy, V., Ed.; VCH: New York, 1991. (b) Ramamurthy, V.; Eaton, D. F. *Acc. Chem. Res.* **1988**, *21*, 300−306. (c) Weiss, R. G.; Ramamurthy, V.; Hammond, G. S. *Acc. Chem. Res.* **1993**, *26*, 530−536. (d) Ramamurthy, V.; Eaton, D. F.; Caspar, J. V. *Acc. Chem. Res.* **1992**, *25*, 299−307. (e) Sivaguru, J.; Natarajan, A.; Kaanumalle, L. S.; Shailaja, J.; Uppili, S.; Joy, A.; Ramamurthy, V. *Acc. Chem. Res.* **2003**, *36*, 509−521.
(3) (a) Turro, N. J. *Acc. Chem. Res.* **2000**, *33*, 637−646. (b) Turro, N. J. *Chem. Commun.* **2002**, 2279−2292. (c) Turro, N. J. *Proc. Natl. Acad. Sci. U.S.A.* **2005**, *102*, 10766−10770. (d) Turro, N. J. *Proc. Natl. Acad. Sci. U.S.A.* **2002**, *99*, 4805−4809. (e) Turro, N. J.; Grätzel, M.; Braun. A. M. *Angew. Chem., Int. Ed. Engl.* **1980**, *19*, 675−696.
(4) (a) Tung, C. H.; Wu, L. Z.; Zhang, P. P.; Chen, B. *Acc. Chem. Res.* **2003**, *36*, 39−47. (b) Gamlin, J. N.; Jones, R.; Leibovitch, M.; Patrick, B.; Scheffer, J. R.; Trotter, J. *Acc. Chem. Res.* **1996**, *29*, 203−209. (c) Toda, F. *Acc. Chem. Res.* **1995**, *28*, 480−486. (d) Zimmerman, H. E.; Nesterov, E. E. *Acc. Chem. Res.* **2002**, *35*, 77−85. (e) Garcia-Garibay, M. A. *Acc. Chem. Res.* **2003**, *36*, 491−498. (f) Whitten, D. G.; Russell, J. C.; Schmehl, R. H. *Tetrahedron* **1982**, *38*, 2455−2487. (g) Whitten, D. G. *Acc. Chem. Res.* **1993**, *26*, 502−509. (h) Weiss, R. G. *Tetrahedron* **1988**, *44*, 3413−3475.
(5) Gibb, C. L. D.; Gibb, B. C. *J. Am. Chem. Soc.* **2004**, *126*, 11408−11409.
(6) (a) Gibb, C. L. D.; Gibb, B. C. *Chem. Commun.* **2007**, 1635−1637. (b) Gibb, C. L. D.; Gibb, B. C. *J. Am. Chem. Soc.* **2006**, *128*, 16498−16499.
(7) Natarajan, A.; Kaanumalle, L. S.; Jockusch, S.; Gibb, C. L. D.; Gibb, B. C.; Turro, N. J.; Ramamurthy, V. *J. Am. Chem. Soc.* **2007**, *129*, 4132−4133.

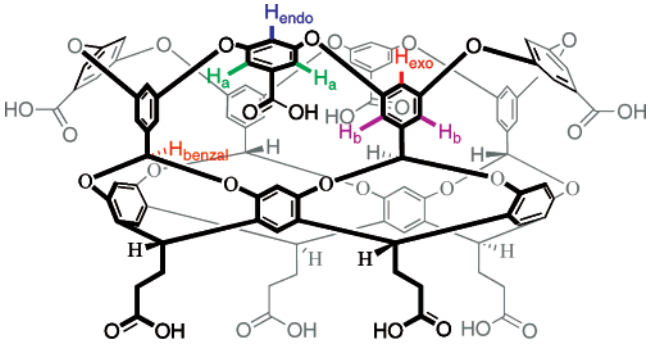

1

We have shown recently that products of oxidation of olefins,[7] geometric isomerization of stilbenes,[8] dimerization of acenaphthylene and styrenes,[8,9] α-cleavage reaction of dibenzyl ketones (DBK),[10] *β*-cleavage reaction of naphthyl esters,[11] and excimer formation of anthracene[12] could be controlled by enclosing photoreactive molecules within the confined space of the capsule. These studies have established the importance of free space and weak interactions between the host interior and the guest molecules in altering the excited-state behavior of the latter. A detailed photochemical investigation of DBK[10] and 1-(4-alkylphenyl)-3-phenyl propan-2-ones (*para*-alkyl DBK) revealed[13] that the extent of free space at the tapered ends of the capsule plays an important role in the extent of rearrangement product formed (Scheme 1, yield of product **9** (R = H) from dibenzyl ketone: 49% and corresponding product from 1-(4-pentylphenyl)-3-phenyl propan-2-ones: 0%).

Formation of **9** from DBK within a capsule is envisioned to proceed as follows: The encapsulated DBK **2** (R = H) is orientated in such a manner that each aromatic ring occupies one cavitand or hemisphere. Upon irradiation, one of the C−C bonds α to the carbonyl group homolytically cleaves, but the resulting radicals do not optimally pack the cavity and thus the benzyl radical rotates 180° relative to the acyl radical. Coupling of the radicals at the para position of the benzyl ring followed by 1,5 H-shift results in **9**.

With these results in hand, and with the idea of expanding on the repertoire of this capsule as a water-based nanoreactor, we sought to investigate the photochemistry of encapsulated α-(*n*-alkyl) DBK derivatives **2a**−**h**, which undergo both Norrish type II and/or Norrish type I reactions. Our interest was to examine how guest packing within the capsule (as dictated by the variable α-*n*-alkyl chain) influenced the partitioning of α-(*n*-alkyl) DBK derivatives **2** by the two reaction pathways. The presence of an α-(*n*-alkyl) group desymmetrizes the guest, and in relation to this study, the two benzyl carbon−carbonyl carbon bonds and the two phenyl rings. In this work, we differentiate between the latter by referring to them as being proximal or distal to the alkyl group (red and blue, respectively, Scheme 1). The study consisted of two parts: (a) a photochemistry section that explores the excited-state chemistry of these guests **2a**−**h**, and (b) an NMR analysis revealing the packing of each guest within the capsule.

Experimental Section

Materials. Host **1** was synthesized according to the literature.[5] The different α-(alkyl) DBK guests were synthesized by the general procedure outlined below (Scheme 2). DBK, sodium hydride, and alkyl bromides were obtained from Aldrich and used as such. THF was freshly distilled over sodium.

Sodium hydride (60% dispersion in mineral oil, 0.6 equiv; washed with dry pentane) was stirred with THF and cooled to 0 °C. DBK (1 equiv, dissolved in THF) was added with stirring. Alkyl bromide (0.6 equiv) was added over 10−15 min, and the reaction was continued at 0−10 °C for 1−1.5 h (40−50% alkylation). The reaction was quenched by slow addition of 10% aqueous NH_4Cl solution. THF was removed under reduced pressure, and the product was extracted with three portions of ether. The ether layer was washed with brine, dried over Na_2SO_4, and concentrated to obtain the crude product as a viscous liquid containing about 5−10% of dialkylated DBK. Purification by flash chromatography (silica gel, hexanes/dichloromethane) afforded the *a*-alkyl DBK as a viscous oil. ^{1}H NMR and ^{13}C NMR data for **2a**−**h** are presented in the Supporting Information.

Protocols for NMR Binding Studies. NMR experiments were performed on an Inova 500 MHz spectrometer (Varian Inc.). All binding studies involved titration of the α-alkyl DBK **2** to the host solution to confirm the stoichiometry of the complexes. The general protocol was as follows: 0.6 mL of 1 mM host **1** and 10 mM sodium tetraborate in D_2O were titrated with aliquots of 2 μL of a 30 mM solution of **2** in DMSO-d_6. Full complexation occurred at 0.5 equiv of **2** (i.e., 10 μL). Complexation was rapid on the experimental time scale, but the NMR spectra were rerecorded after 24 h to ensure no further changes had occurred.

To perform COSY, TOCSY (mixing time 80 ms), and NOESY (mixing time 0.5 s) experiments, 5 mM solutions of the complexes were prepared: 5 mM host **1**, 2.5 mM α-alkyl DBK **2** (R = various), and 50 mM sodium tetraborate in D_2O. Variable-temperature ^{1}H NMR experiments ranged from 5 to 60 °C.

Protocols for NMR Diffusion Measurements. Diffusion measurements were performed on an Inova 500 MHz (Varian Inc.) instrument equipped with a Performa II pulsed field gradient (PFG) module capable of producing pulses up to 52 G/cm. The experiments were carried out on a 5-mm PFG indirect detection probe. The stimulated echo (STE) diffusion experiment using the Varian pulse sequence "pge" (stimulated option on) was performed with pulse gradients of 2 ms in duration separated by 155 ms. Calibration utilized D_2O samples with a diffusion constant of 1.88 10^{-5} cm^2 s^{-1}. The experiments were performed at 25 °C, at a host concentration of 1 mM (in 10 mM sodium tetraborate). The given diffusion constants were an average of three measurements. Data were analyzed using the optional Varian diffusion software and gave, for example, a value of $D = 1.82\ 10^{-6}$ cm^2 s^{-1} for the free host **1** and a value of $D = 1.30\ 10^{-6}$ cm^2 s^{-1} for the **2 a@1** complex. Assuming the entity is spherical, a hydrodynamic radius (R_h) and corresponding volume can be calculated from D according to the following equation:

$$R_h = \frac{kT}{6\pi\eta D}$$

where R_h is the hydrodynamic radius of the sphere in meters, k is the Boltzmann constant, T is the temperature in Kelvin, η is the solvent viscosity, and D is the diffusion constant in m^2 s^{-1}.

Protocols for Photochemistry Experiments. Irradiations were carried out using a medium-pressure Hg lamp. All samples were bubbled with N_2 for 30 min before irradiations, and bubbling continued during photolysis. Solutions of the ketones **2a**−**h** (10^{-3} M) in hexanes

(8) Parthasarathy, A.; Kaanumalle, L. S.; Ramamurthy, V. *Org. Lett.* **2007**, *9*, 5059−5062.
(9) Kaanumalle, L. S.; Ramamurthy, V. *Chem. Commun.* **2007**, 1062−1064.
(10) Kaanumalle, L. S.; Gibb, C. L. D.; Gibb, B. C.; Ramamurthy, V. *J. Am. Chem. Soc.* **2004**, *126*, 14366−14367.
(11) Kaanumalle, L. S.; Gibb, C. L. D.; Gibb, B. C.; Ramamurthy, V. *Org. Biomol. Chem.* **2007**, *5*, 236−238.
(12) Kaanumalle, L. S.; Gibb, C. L. D.; Gibb, B. C.; Ramamurthy, V. *J. Am. Chem. Soc.* **2005**, *127*, 3674−3675.
(13) Sundaresan, A. K.; Ramamurthy, V. *Org. Lett.* **2007**, *9*, 3575−3578.

Scheme 1. Overall Reaction Manifold for the Photochemistry of Encapsulated DBK and α-Alkyl DBKs[a]

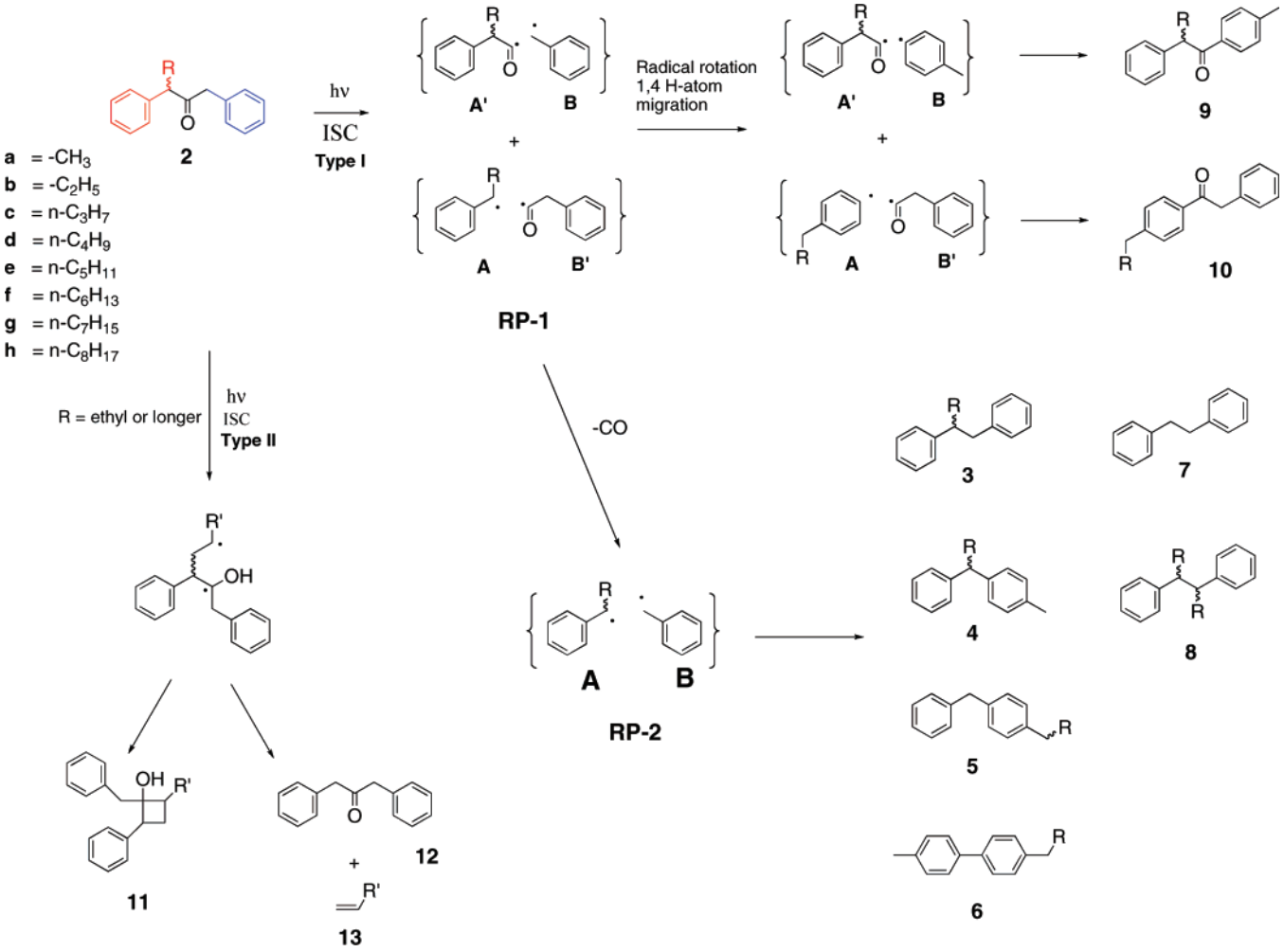

[a] The three routes away from starting material are: (1) Norrish type I photochemistry that leads to (a) a range of decarbonylated products **3**−**8** and (b) rearranged products **9** and **10**, and (2) Norrish type II photochemistry to yield products **11**−**13**. In structures **11** and **13**, R′ represents alkyl chain that is less by CH_2CH_2 from R.

or aqueous sodium tetraborate (10^{-2} M) taken in a Pyrex test tube were irradiated for 30 min. Reaction conversion of 30−50% was achieved during this period. The products (extracted from buffer solution using $CHCl_3$) were analyzed by GC (HP 5890 series, SE-30 column) and GC−MS (HP-6890N with 5975B MSD; HP-5 column).

A stock solution of cavitand **1** (10^{-3} M) was prepared in sodium tetraborate (10^{-2} M) buffered H_2O or D_2O. Stock solutions of the guests were prepared in DMSO-d_6. To 0.6 mL of a solution of **1** taken in an NMR tube, an aliquot of guest solution was added, maintaining a host−guest ratio of 4:1, and the solution was sonicated for 30 min. ^{1}H NMR showed formation of complex. The complex was irradiated for 30 min, maintaining nitrogen purge during irradiation. The products were extracted using chloroform and analyzed by GC and GC−MS. Photoproducts were identified by comparison with those obtained from irradiation of homogeneous solutions. Structures of rearrangement products (**8** and **9**) were established by comparison with authentic samples prepared independently.

Results

Stoichiometry of the Complexes. Eight guests, α-methyl- through α-(*n*-octyl) DBK (Scheme 1, **2a**−**h**), were examined. ^{1}H NMR titration studies involving **1** and **2** revealed that all formed capsular 2:1 host−guest complexes. The significant upfield shift (vide infra) of the guest signals revealed that all were held within the essentially dry interior of the capsule. Low concentrations of free guest were apparent when the titration went beyond stoichiometric, demonstrating that guest exchange between the free and encapsulated environments was slow on the (500 MHz) NMR timescale. Confirmation of the capsular nature of these complexes was also obtained using pulse gradient spin−echo NMR experiments,[14] which yielded the diffusion rates and corresponding particle sizes (Table 1).

Scheme 2. Synthesis of the Different α-(Alkyl) DBK Guests

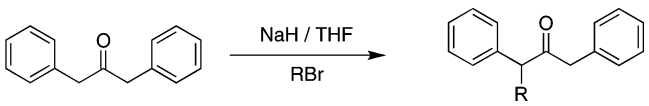

Photochemical Results. In general, α-(*n*-alkyl) DBKs undergo two types of photoreactions: Norrish type I and type II (Scheme 1). The second reaction occurs only with guests that possess γ-hydrogen atoms (**2c**−**h**). Our primary interest was to explore the photochemical behavior of these molecules when included in the capsule formed by **1**. For comparative purposes, their excited-state behaviors in hexane and borate buffer were also investigated. Results of photolysis are summarized in Table 2. As expected, irradiation of ketones **2a** and **2b** in hexane and

(14) Cohen, Y.; Avram, L.; Frish, L. *Angew. Chem., Int. Ed.* **2005**, *44*, 520−554.

Table 1. Diffusion Rates, Complex Radius, and Volume for the Complexes Formed between **2a**−**h** and **1** as Derived from Pulse Gradient Spin−Echo NMR Spectrometry

guest (**2**, R =)	diffusion rate ($\times 10^{-10}$ m^2 s^{-1})	hydrodynamic radius[a] (nm)	hydrodynamic volume[b] (nm^3)
CH_3	1.30	1.7	19.8
C_2H_5	1.33	1.6	18.5
n-C_3H_7	1.28	1.7	20.8
n-C_4H_9	1.32	1.7	18.9
n-C_5H_{11}	1.32	1.7	18.9
n-C_6H_{13}	1.46	1.5	14.0
n-C_7H_{15}	1.27	1.7	21.3
n-C_8H_{17}	1.31	1.7	19.4

[a] Derived from Rh (hydrodynamic radius) = $kT/(6\pi\eta D)$. [b] Derived from $V = 4/3\pi r^3$ (R = Rh).

Table 2. Product Distribution upon Photolysis of α-(*n*-Alkyl) Dibenzyl Ketones in Hexane and Borate Buffer and as Complexes with the Capsule in Borate Buffer[a,b]

guest **2**		type 1					type 2	
					rearranged DBK			
	medium	AA (**7**)	AB[c] (**3**)	BB (**8**)	(**9**)	(**10**)	DBK (**12**)	cyclobutanol (**11**)
2a	hexane	24	48	28	0	0		
	buffer	21	53	26	0	0		
	capsule		75		4	21		
2b	hexane	23	48	29	0	0		
	buffer	23	50	27	0	0		
	capsule	7	51	8	5	29		
2c	hexane	16	40	24	0	0	11	9
	buffer	16	43	21	0	0	11	9
	capsule		50		4	35	4	7
2d	hexane	17	45	20	0	0	7	11
	buffer	17	52	18	0	0	7	6
	capsule	0	29	0	28	36	2	5
2e	hexane	16	41	23	0	0	4	16
	buffer	17	46	26	0	0	4	7
	capsule	0	28	0	34	32	3	3
2f	hexane	15	46	32	0	0	4	3
	buffer	14	51	27	0	0	6	2
	capsule	0	73	0	0	0	25	2
2g	hexane	13	49	26	0	0	4	8
	buffer	15	49	26	0	0	4	6
	capsule	0	60	0	0	0	32	8
2h	hexane	16	46	23	0	0	5	10
	buffer	13	42	20	0	0	20	5
	capsule	0	10	0	0	0	83	7

[a] See Scheme 1 for structures of products. [b] The GC results are average of at least six independent runs, and reported yields are based on the integrated area of the GC signals. [c] Includes AB **3** and its isomers **4**, **5**, and **6**.

borate buffer resulted in 1,3-diphenyl ethanes **7** (AA), **3** (AB), and **8** (BB) in 1:2:1 ratios. Furthermore, excitation of **2c**−**h** possessing γ-hydrogen atoms gave products of both Norrish type I and type II reactions. On the other hand, irradiation of the 2:1 complexes formed between host **1** and guests **2a**−**h** gave a distribution of products strikingly different from that in solution. Trends observed were: (a) Irradiation of seven α-alkyl DBKs (**2a**, **2c**−**h**) did not give the cage escape products **7** and **8** (AA and BB). The only decarbonylated products obtained from these were AB and its rearrangement isomers (**3**−**6**). α-Ethyl DBK (**2b**) gave small amounts of AA and BB along with major amounts of AB. (b) On the basis of their photobehavior, we can divide the eight guests into three groups. The first consists of α-hexyl, α-heptyl, and α-octyl DBKs (**2f**−**h**) that do not give any rearranged starting ketones either in isotropic solution or within the capsule. These ketones yield large amounts of Norrish type II products within the host. This was especially true with encapsulated α-octyl DBK that gave 90% of Norrish type II products, **11** and **12**, while in hexane solution the predominant products (~85%) were from Norrish type I reaction. (c) The second group consists of α-butyl and α-pentyl DBKs (**2d** and **2e**) that yield the two rearranged starting ketones **9** and **10** in major amounts (>60%) almost in equal ratio. Products of Norrish type II reaction were obtained in less than 10% yield. (d) The third group consists of α-methyl, α-ethyl, and α-propyl DBKs (**2a**−**c**) that within capsule yield only one (not two) rearranged starting ketone **10** in larger amounts. The second one (**9**) is formed in less than 5%. In this set, as expected, only α-propyl DBK gave Norrish type II products.

^{1}H NMR Structural Characterization of Host−Guest Complexes. This section is subdivided into three parts pertaining to signals from the alkyl chain of the guest, the guest aromatic region, and the host aromatic region. Characterization relied on signal shift data in the 1D spectrum (the general rule is that atoms residing at the tapered top and bottom regions of the capsule are shifted more from the free state than those residing at the equatorial region), as well as COSY, TOCSY (short- and long-range coupling within the guest), and NOESY (through-space host−host, guest−guest, and host−guest interactions) experiments. With the exception of Figures 2−4, all these data are presented in the Supporting Information.

Alkyl Chain NMR Data. Figure 1 reveals that the α-alkyl chain signals (numbered such that the terminal methyl groups are labeled H_1) appear in the upfield region of the ^{1}H NMR. The shift in the methyl signal of **2a** upon complexation ($\Delta\delta$ = −0.98 ppm) is relatively small. However, the corresponding shifts increased with lengthening alkyl chain: **2b**, −1.82 ppm; **2c**, −2.79 ppm; **2d**, −3.72 ppm; **2e**, −3.79 ppm; **2f**, −3.66 ppm; **2g**, −3.97 ppm; and **2h**, −4.07 ppm. Within the confines of the capsule, most of the methylene hydrogens were observably diastereotopic, with two signals for almost all methylene groups. However, some signal overlaps were apparent in longer homologues (**2f**−**h**). In almost all cases, the methylene hydrogens β to the carbonyl chromophore demonstrated the largest anisotropy. For guests **2c**−**h**, NOESY NMR revealed through-space interactions between the host H_{benzal} atoms (see **1**) and the terminal methyl. For the longer homologues, **2e**−**h**, an interaction between the H_{benzal} atoms and the penultimate methylene was also observed. This latter point suggests that packing is such that the methyl group is anchored deeply in the tapering cavity of the cavitand.

Aromatic Signals of the Guest. For convenience, we label the two aromatic rings of the guest as proximal and distal to the R group (red and blue, respectively, in Scheme 1). In the case of **2a**, all six signals for the two rings were visible as pairs at $\delta \approx 5.50$ ppm (2H each), 4.70 ppm (2H each), and 3.50 ppm (1H each). Confirmation of their identity required both COSY and TOCSY NMR. The COSY spectrum identified several key interactions within the guest, including the methyl−methine coupling, both ortho−para couplings, and one of the meta−para couplings. In regards to the latter, both meta−para couplings were apparent with TOCSY NMR. Taken together, these data identified the pairs of signals at $\delta \approx 5.50$, 4.70, and 3.50 ppm as belonging to the *ortho*-, *meta*-, and *para*-hydrogens, respectively, of the two phenyl rings. The NOESY NMR spectrum of the complex revealed many interactions, including those between the *para*-hydrogens of the guest and the H_{benzal}

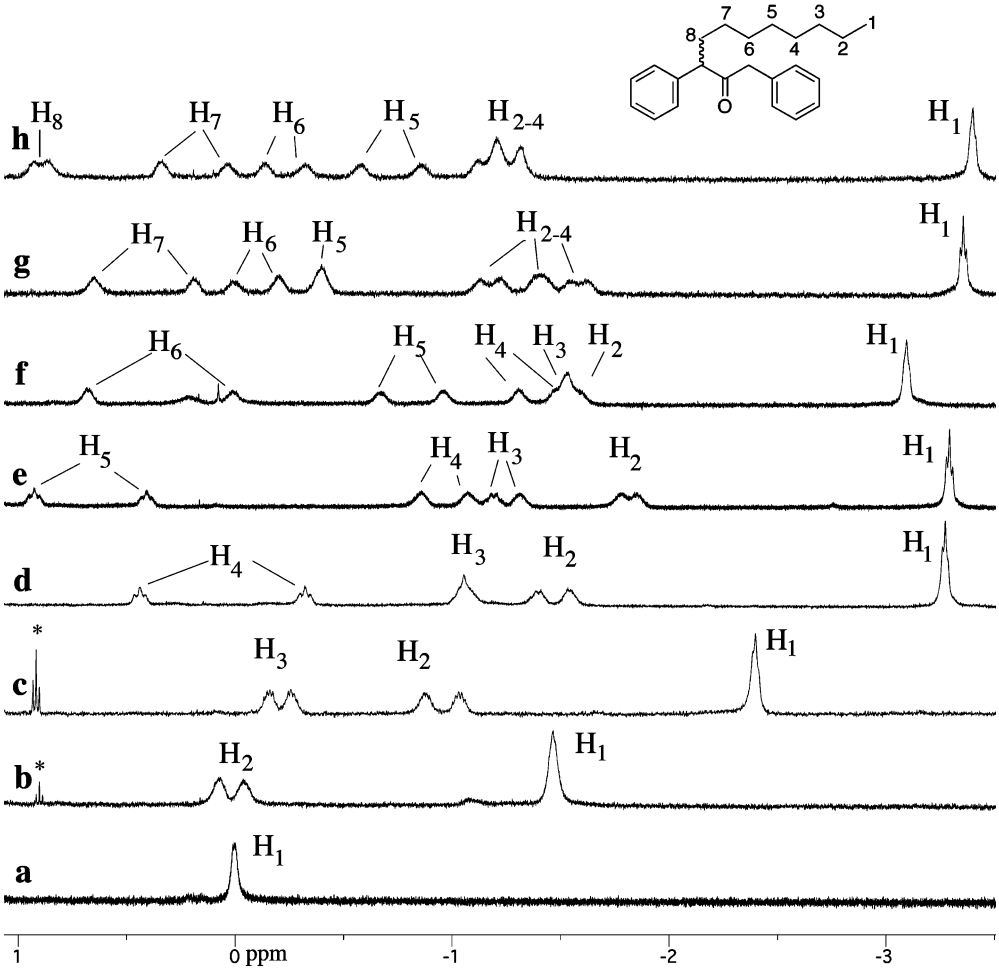

Figure 1. Guest region of the ^{1}H NMR spectra of the complexes formed between cavitand **1** and α-alkyl DBK guests **2a**−**h**. Guests are: (a) **2a**, (b) **2b**, (c) **2c**, (d) **2d**, (e) **2e**, (f) **2f**, (g) **2g**, and (h) **2h**. Numbering is such that the methyl group is position one. Numbering for **2h** is shown as an example. * Denotes impurity.

atoms of the host. A similar situation was observed with the complex of **2b**. The α-propyl DBK (**2c**) complex behaved slightly differently. In this complex, one set of aromatic signals was considerably more shifted that the other, confirming that one ring was not located deep in a hemisphere but rather in the equatorial region of the capsule. The presence of an NOE interaction between the *ortho*-hydrogens of this ring and the methine hydrogen identified it as the proximal (to the R group) phenyl. Only five of the six aromatic ring signals for encapsulated **2d** were observed. The ring with only two signals accounted for was the least shielded, and as was the case for the complex with **2c**, this was assigned as the proximal ring. In contrast to the smaller homologues, signals from only one aromatic ring were observable in the complex with **2e**. The observable ring was shielded to a slightly greater extent than the most shielded ring in the **2d** complex and showed no NOE between its *ortho*-hydrogen atoms and the methine C−H. Again, therefore, this deeper phenyl was assigned as the distal ring. For encapsulated **2f**, only two aromatic signals from the guest were apparent. COSY and TOCSY NMR revealed no coupling between these, suggesting that they are not in the same ring (or, less likely, that the dynamic nature of the encapsulated guest masked coupling). In the **2g** complex, four aromatic signals of the guest were visible, but COSY NMR did not yield coupling information. However, TOCSY NMR did identify that the signals at 2.80 and 5.10 ppm belong to the same ring. Additionally, integration confirmed that the former corresponded to a *para*-hydrogen, while an NOE interaction between the latter and the methine hydrogen of the guest confirmed that this signal originated form the *ortho*-hydrogens of the proximal phenyl. Finally, in the **2h** complex the two phenyls of the guest were again observed: one bound deeply, the other shielded only to a small amount. The *ortho*-hydrogens of the deeply bound ring showed an NOE interaction with the methine H of the guest, again demonstrating that it was the proximal ring.

Aromatic Signals of the Host. As the guests **2a**−**h** are chiral, the enantiotopic host atoms H_a and H_b (**1**) are diastereotopic (nonequivalent) in the complex. However, with the complexes of **2a** and **2b**, only the signals for the H_a atoms were observed to be magnetically nonequivalent; a singlet was observed for the H_b atoms (Figure 2). It is not clear why in this case the H_a atoms on the exterior of the host are better reporters for the encapsulation of chiral guests than the H_b atoms that make up part of the wall of the cavity. In the complex with **2c**, the anisotropy of the diastereotopic H_a atoms was diminished (Figure 2c) and the formally diastereotopic H_b atoms continued to be indistinguishable. In contrast, the NMR spectra of the complexes with **2d** and **2e** (Figures 2d and 3a) revealed the diastereotopicity of not only the H_a atoms, but also the H_b atoms. However, in the **2f** complex the nonequivalence of the H_a atoms

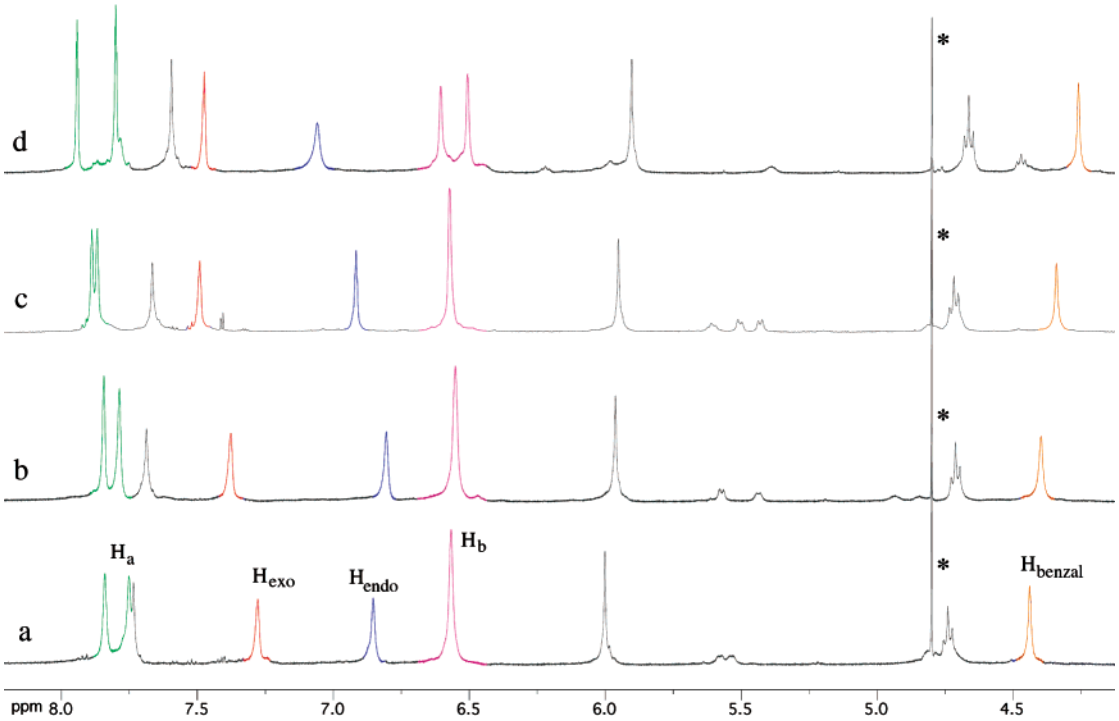

Figure 2. Aromatic region of ^{1}H NMR spectra of the complexes formed between cavitand **1** and guests **2a**−**d**. R guests are: (a) **2a**, (b) **2b**, (c) **2c**, and (d) **2d**. * Denotes residual water signal.

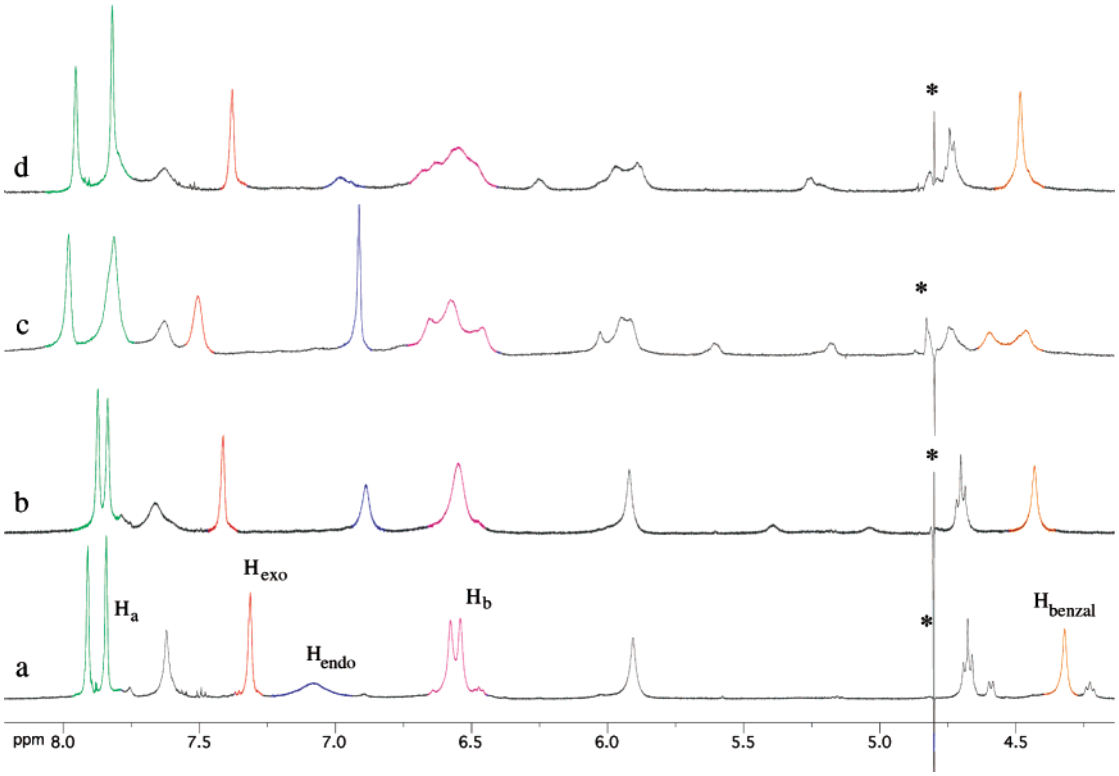

Figure 3. Aromatic region of ^{1}H NMR spectra of the complexes formed between cavitand **1** and guests **2e**−**h**. Guests are: (a) **2e**, (b) **2f**, (c) **2g**, and (d) **2h**. * Denotes residual water signal.

is diminished, and only a broad signal for the H_b atoms is apparent. The NMR signals due to the host in the complex with **2g** are interesting; the host signals, which undergo relatively small shifts upon complex formation, were broadened in this complex (Figure 3c), presumably because of the reduced mobility of this larger guest. Nevertheless, it was still possible to identify two H_a signals, and for the first time two H_{benzal} signals. Increased temperature leads to increased mobility, and the NMR spectrum of this complex at 60 °C was more akin to those of the smaller homologues (Figure 4a). Correspondingly,

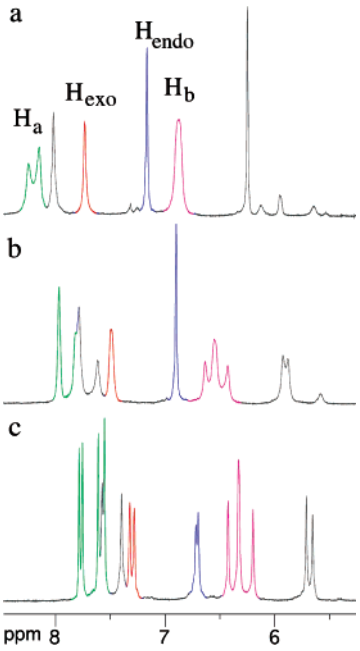

Figure 4. Variable-temperature ^{1}H NMR spectra of the complex formed between cavitand **1** and guest **2g**. Temperatures are: (a) 60, (b) 25, and (c) 5 °C.

at a relatively low 5 °C tumbling of the guest whereby the contents of each hemisphere exchange places was slow on the NMR time scale, with the result that the host signals underwent splitting (Figure 4c). The NMR host signals of the complex with **2h** are also generally broad at room temperature (Figure 3d). However, in contrast to the **2g** complex, the H_{benzal} signal is not split. Variable-temperature studies gave results analogous to the **2g** complex.

Discussion

In aqueous solution, host **1** dimerizes around a broad range of molecules.[5−12] In the study here, a series of eight α-(*n*-alkyl) DBK derivatives **2a**−**h** yielded 2:1 capsular complexes (**2a**−**h**@**1**$_2$). The first part of this section is devoted to determining the structures of these complexes using NMR. The second part discusses the photochemistry of these different complexes. It is satisfying to note that the NMR-derived structures of the guests within the capsule remarkably predict the observed photochemical behavior of the guest ketones.

Structural Characterization of the Host−Guest Complexes through ^{1}H NMR. Characterization by NMR relied on 1- and 2D experiments. In the former, a comparison between the spectra of the free host and guest and the corresponding complex is useful because the binding pocket of each cavitand is akin to a truncated cone. Hence, atoms that reside deeper in the cavity are more shifted (shielded) by the aromatic wall of the capsule than those that are located at the equator. This phenomenon is par for the course for resorcinarene-based hosts and capsules.[5−12,15−21] Additionally, for full characterization it was necessary to collect COSY (short-range coupling), TOCSY (long-range coupling), and NOESY (through-space host−host, guest−guest, and host−guest interactions) data.

As we shall see, NMR revealed three guest-packing motifs modulated by the length of the α-alkyl chain of the guest. To define these different packing motifs, we define two distinct regions within the capsule and three moieties of the guest. Thus, the capsule has two identical polar regions and an equatorial region, while the guests are viewed in terms of the variable R group and the phenyl rings proximal (red in Figures 1 and 5) and distal (blue) to the R group. We observed three packing motifs: the two aromatic rings occupy the polar region of the capsule and the R group the equatorial region (e.g., Figure 5a); the distal phenyl and R group occupy the polar regions (e.g., Figure 5d); and the proximal phenyl and the R group occupy the polar regions (e.g., Figure 5h).

(1) Guests that Pack the Two Hemispheres with Two Aromatic Rings. Packing of guests **2a** and **2b** is dominated by their aromatic rings. Multiple lines of evidence from NMR confirm that for **2a** and **2b** each phenyl ring occupies a hemisphere (Figure 5a,b). Thus, the methyl groups of **2a** and **2b** are shifted −0.98 and −1.82 ppm, respectively, from their free states (Figure 1). These are relatively small shifts compared to the ca. 4.00 ppm shifts of the larger homologues, suggesting that their R groups are located in the spacious equatorial region of the capsule. However, no NOE interactions between these methyl groups and the suitably located H_{endo} atoms of the host were observed. The shift in the methyl signal of **2c** is larger (−2.97 ppm) and in contrast shows an NOE interaction with the inward point H_{benzal} atoms of the host. In combination, these data suggest that the side chain of the propyl guest is beginning to compete with one of the aromatic rings for occupation of a hemisphere (Figure 5c). Remaining with the alkyl groups of these guests, it is worth noting that the CH_2 groups are observably diastereotopic. The anisotropy *within* a CH_2 group is small and consistent, while the anisotropy *between* the CH_2 and the terminal methyl is large.

The proposed structures for the three complexes are also supported by the aromatic signals of each guest. For **2a** and **2b**, both phenyls undergo significant shifts relative to the free state. All six signals are apparent in both complexes, and a combination of COSY and TOCSY experiments confirmed that the *ortho*-, *meta*-, and *para*-hydrogens of both rings occur in pairs at ca. 5.5, 4.7, and 3.5 ppm. It is the *para*-hydrogens that are the most deeply bound, a conclusion further supported by NOE interactions between the *para*-hydrogens of each guest and the H_{benzal} atoms of the host. In contrast, in the complex with **2c** only one aromatic ring is markedly shielded. The other ring is much less so, suggesting that its average position is closer to the equatorial region. Indeed, CPK models confirm that there is little room for both the propyl side chain and an aromatic ring to occupy a hemisphere. Which aromatic ring is displaced toward the equator? The *ortho*-hydrogens of the aromatic ring experiencing less shielding show strong NOEs with the methine hydrogen of the guest and the adjacent methylene group on the side chain, confirming that it is the proximal aromatic rings that are being displaced from the hemisphere by the propyl group (Figure 5c). The propyl group is less voluminous than the phenyl ring (69 versus 98 Å^3), but it presumably packs the narrowest part of the cavity more efficiently. These points stated, comparing the NMR data and photochemical products from this

(15) Biros, S. M.; Rebek, J., Jr. *Chem. Soc. Rev.* **2007**, *36*, 93−104.
(16) Rebek, J., Jr. *Angew. Chem., Int. Ed.* **2005**, *44*, 2068−2078.
(17) Purse, B. W.; Rebek, J. J. *Proc. Natl. Acad. Sci. U.S.A.* **2005**, *102*, 10777−10782.
(18) Rebek, J., Jr. *J. Org. Chem.* **2004**, *69*, 2651−2660.
(19) Hof, F.; Rebek, J., Jr. *Proc. Natl. Acad. Sci. U.S.A.* **2002**, *99*, 4775−4777.
(20) Rebek, J., Jr. *Chem. Commun.* **2000**, 637−643.
(21) Rebek, J., Jr. *Acc. Chem. Res.* **1999**, *32*, 278−286.

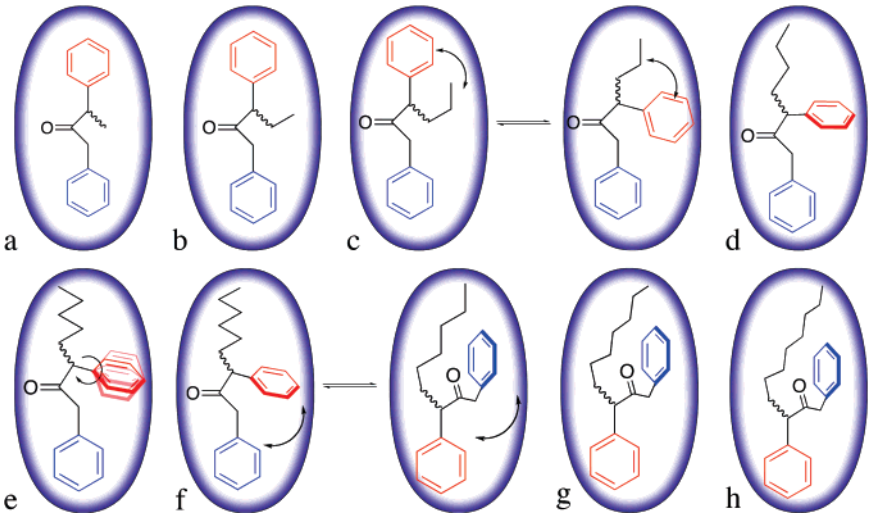

Figure 5. Representations of the complexes formed by: (a) **2a**, (b) **2b**, (c) **2c**, (d) **2d**, (e) **2e**, (f) **2f**, (g) **2h**, and (h) **2h**.

complex to those formed by **2d** and **2e** (vide infra) suggests that the equilibrium between the two states depicted in Figure 5c is in favor of the phenyl ring occupying the northern hemisphere.

Guest packing changes are also evident in the NMR signals of the host. Such changes can be illustrated using the atoms (see structure **1**) H_a, H_b, H_{endo}, H_{exo}, and H_{benzal} (Figure 2). In regards to changes in absorption, the inward pointing H_{benzal} atoms are good reporters of guest binding. In the case at hand, there is an upfield shift in this signal as the alkyl group changes from methyl to *n*-propyl, a trend that continues through to the complex **2d**. Host signal splitting is also informative. Formally, atoms H_a and H_b are enantiotopic in the free host and diastereotopic in the complexes. Interestingly, however, the atoms more remote from the chiral guest (H_a) are better reporters for encapsulation than the H_b atoms that make up part of the wall of the cavity. Although slightly more removed from the binding site, changes to their surrounding environment upon guest binding are apparently more significant.

In summary, guests **2a**−**c** pack the capsule such that the two aromatic rings occupy the two hemispheres. However, with guest **2c** the propyl group competes with the proximal phenyl ring for packing a hemisphere.

(2) Guests that Pack the Hemispheres with an Alkyl Group and the Distal Ring. Whereas the alkyl group in the **2c** complex struggles for occupancy of the northern hemisphere, NMR evidence demonstrates that those of the **2d** and **2e** complexes are large enough (87 and 105 Å^3, respectively) to fully displace the proximal phenyl ring (98 Å^3). Thus, the methyl shift in these two complexes is near maximal (−3.72 and −3.79 ppm, respectively). These greater shifts can be attributed to two phenomena: a longer residency time in the hemisphere and occupation of deeper/narrower regions of the cavity. The latter is particularly evident in the NOESY NMR spectrum of the complex with **2e**, which shows NOEs between the H_{benzal} atoms of the host and both the terminal methyl and the penultimate methylene group. The chain is now long enough that the methyl group can move beyond the crown of H_{benzal} atoms.

For both guests, the alkyl group methylene signals are distributed over a range of ca. 4 ppm. There is therefore no signal coincidence and it is possible to observe the large anisotropy of the respective H_4 and H_5 atoms in the complex with **2d** and **2e** (Figure 1). Apparently, one of these diastereotopic pairs is considerably more shielded than the other. Presumably, it lies close to, and close to the plane of, the proximal phenyl ring.

For **2d**, only five of the six aromatic signals are apparent in the complex. The ring with all three observable signals was the most shielded and, following on from the complex with **2c**, was assigned as the distal phenyl. Another difference between the aromatic signals of **2d** and encapsulated **2c** was the degree of shielding of this distal ring. It was not possible to fully assign all the signals of free guest in aqueous solution and therefore not possible to accurately determine the corresponding $\Delta\delta$ values for both complexes. Nevertheless, the −0.60 ppm shift for the *para*-hydrogen in encapsulated **2d** versus the **2c** complex is much larger than any difference between the free guests. Hence, the increased size of the alkyl group forces the distal phenyl deeper into the opposing hemisphere.

The complex with **2e** proved to be less informative; no signals for the less shielded, equatorial, proximal ring were apparent. Furthermore, variable-temperature studies (5−55 °C) failed to yield any information about this "invisible" ring. As it "reappears" in the larger complexes (vide infra), a dynamic conformational process on or near the NMR time scale is assumed to be behind this phenomenon. Figure 5e denotes, by way of example, a slowed rotation around the C−Ph bond.

Changes in packing are also indirectly observable in the NMR spectrum of the host. For example, following a decreasing trend in anisotropy of the H_a atoms in the complexes with **2a** to **2c**, there is a sudden increase (Figure 2) in their diastereotopicity in the complex with **2d**. Furthermore, it is possible for the first time to observe magnetic nonequivalence for the H_b atoms, atoms that, although formally diastereotopic, appear equivalent in the complexes of **2a**−**c**. Interestingly, the complex with **2e** again reveals the diastereotopicity of these atoms (Figure 3), but the anisotropy in both is diminished relative to that of **2d**.

One interesting feature of the host region of the complex with **2e** is broadening of the H_{endo} signal (Figure 3). These eight atoms in the complex point inward at the equatorial region of the capsule and are good reporters of events at the region. It will become apparent (vide infra) that gross flipping of the guest within the capsule, whereby the contents of one hemisphere trade places with the contents of the other, slows down to the NMR

time scale as the guest increases in size. However, such broadening occurs for all host signals. For the **2e** complex, only the H_{endo} signal broadens, and with the bigger guests this peak is sharper. In other words, this H_{endo} broadening is out of step both with other signals from this complex and with H_{endo} signals in different complexes. We attribute this manifestation to the same (on the NMR time scale) movement responsible for the "missing" aromatic ring. Again, variable-temperature studies do not reveal more information about this process, but we view it as quite distinct from the global movements of the guest such as gross flipping.

In summary, guests **2d** and **2e** pack the capsule such that the hemispheres are filled with the alkyl group and the distal ring. In this packing arrangement, the proximal ring can adopt one of at least two isoenergetic positions.

(3) Guests that Pack the Hemispheres with an Alkyl Group and the Proximal Ring. NMR data reveal that guests **2f**−**h** pack the cavity of the capsule so that the alkyl group and the proximal ring fill the two hemispheres, while the distal ring resides in the equatorial region of the host. NMR also reveals that, like the guest **2c**, guest **2f** lies on the border between two modes of packing.

The methyl group of the encapsulated **2f** is slightly less shifted (−3.66 ppm) than those of guests **2d** and **2e**. Indeed, this shift is slightly less (Figure 1) than larger guests, suggesting that **2f** is unusual. As with the other guests, all the signals of the *n*-alkyl chains of encapsulated **2f**−**h** can be accounted for. However, packing is tight and there is signal overlap for the H_2−H_4 atoms. This is also apparent with CPK models, which suggest that these guests can fit only if their alkyl chains adopt highly compact conformations. The fact that there is overlap of the alkyl signals, and that accompanying COSY data are incomplete, means that the H_2−H_4 assignments are based on the trends observed for the smaller guests. Nearer the capsule equator, the readily identifiable H_6 and H_7 hydrogens of the *n*-hexyl and *n*-heptyl chains again demonstrate an anisotropy much larger than those other groups in their chain. However, guest **2h** bucks this trend.

Although it is not possible to fully assign the H_2−H_4 atoms of these three guests, the NOE spectrum does provide some intriguing information concerning the general packing of the side chains; for each guest, NOEs are observed in two distinct packets. For example, in the case of the encapsulated **2g**, there are NOEs between atoms H_5−H_7 (0.5 to −0.5 ppm range), a second packet of NOEs between atoms H_1−H_4 (−1.0 to −2.0 ppm), but no interactions between these two groups. It is difficult to envision a conformation in which there is no possibility of NOEs between, for example, H_4 and H_5 and H_6. We therefore attribute this observation to dynamics; conformational changes within each of the two sections of chain allow observation of NOE signals, but movement around the "hinge" section between them is such that intersection NOEs are weak. Returning to the bunching of the signals from H_2−H_4, it would appear that these atoms are situated at a similar depth in the cavity. Thus, a possible packing motif for this chain would be an anchored methyl, three CH_2 groups filling the next level of the cavity, and a "kink" to accommodate the rest of the chain lying at the equator.

As was the case with the **2e** complex, the **2f** complex provides little information from its aromatic rings. Only two signals were observed, and neither COSY nor TOCSY revealed coupling between them. This point notwithstanding, photolysis of this complex and NMR data from the complexes of **2g** and **2h** (vide infra) suggest that the **2f** complex represents the transition between different packing motifs, a packing motif in which the aromatic rings exchange positions with each other (Figure 5f). Thus, now that the alkyl group is sufficiently long, it is energetically feasible to locate the proximal ring in the opposite hemisphere and the distal ring at the equator. The net effect of this change is to make the guest a bit shorter (by $-CH_2C(O)-$), but slightly more rotund (by the same amount). This dynamic nature likely destabilizes the capsule leading to fast diffusion data (Table 1).

For encapsulated **2g**, four of the six aromatic signals are apparent. A COSY experiment did not yield coupling information, but a TOCSY experiment did identify the signals at 5.1 and 2.8 ppm as originating from the same ring. From the studies of the smaller guests, these signals can be attributed to the ortho and para atoms of a hemispherically bound (rather than equatorially bound) aromatic ring. Importantly, the signal at 5.1 ppm showed a strong NOE with the methine hydrogen of the guest, indicating that the most deeply bound phenyl is the proximal ring. This type of interaction was observed with the complex of **2c**, but in that instance the proximal ring was located at the equatorial region; the proximal and distal rings have traded places.

This greater amount of data relative to **2f** suggests that the local, dynamic guest movement of **2g** is slower, and/or that the equilibrium suggested for **2f** (Figure 5f) is pushed more toward the isomer in which the proximal phenyl is embedded in the "southern" hemisphere (Figure 5g). The NMR data for guest **2h** continue this trend. Thus, all six aromatic signals of the guest are observed, and it is apparent that one ring is bound deeply in the southern hemisphere while the other is shielded only to a small amount. As with the **2g** complex, an NOE is observed between the methine H and the *ortho*-hydrogen atom of the deeply embedded proximal ring.

In addition to the changes to the local dynamics identified through the aromatic signals of the guests **2f**−**h** are changes at the next level of scale. These are best illustrated by the aromatic signals of the host. For all the complexes, the host exerts more of an influence on the NMR spectrum of the guest than vice versa. In other words, the host signals undergo relatively small shifts upon complex formation. As a result, slowing of guest tumbling is observed with the broadening of signals from atoms such as H_a, H_b H_{endo}, and H_{exo}, while the guest signals remain well defined ($k_{coal} = \pi\sqrt{2}\Delta\nu$). The broadening of the signal from H_b as the guest increases in size is typical (Figure 3a−d). The effects of temperature upon guest flipping are as expected and are illustrated by the complex with **2g** (Figure 4). At higher temperature, the signals sharpen up somewhat to give a spectrum reminiscent of the smaller guests, whereas at lower temperatures there is considerable splitting of the signals to give a spectrum similar to that observed when rigid guests such as steroids are encapsulated.[3] This "freezing" of guest mobility means that with the exception of diastereotopic atoms H_a and H_b, all the host signals split into sharp doubles; the northern and southern hemispheres are magnetically nonequivalent, and each set of atoms in one hemisphere is heterotopic with respect to its counterpart in the other. This north−south divide also applies to the H_a and H_b atoms. In addition however, because the guests

are chiral, each set of eight H_a/H_b atoms in a hemisphere is split into two magnetically dissimilar (diastereotopic) sets of four atoms. The resulting splitting of splitting is illustrated with H_a; four signals are apparent at 5 °C.

Whereas the aromatic signals of the host follow a systematic broadening as the capacity of the capsule is approached, the H_{benzal} signal remains relatively sharp except in the case of guest **2g** (Figure 3). This unique case of broadening cannot be attributed to the small shift that it undergoes relative to the free host; the shift of the (broad) H_{benzal} of the complex with **2g** is more than the shift of the corresponding (sharp) signal in the **2h** complex. Rather, we suggest that the H_{benzal} of the former is broad because tumbling is slowing down to the NMR time scale, but that the tumbling of the latter is faster because packing is beyond optimal and the two hemispheres of the capsule cannot close properly. Tumbling is still, however, slow enough to cause broadening of the aromatic signals.

To recap, these larger guests adopt a well-defined packing arrangement in which the alkyl group and the proximal phenyl ring fill the hemispheres; it is the distal ring that fills the equatorial regions of the capsule. In contrast, guest **2f** lies at the cusp between the two packing modes demonstrated by **2e** and **2g**.

Effect of Supramolecular Conformational Control on the Excited-State Behavior of α-(*n*-Alkyl) Dibenzyl Ketones. The NMR data discussed above reveal that (a) all ternary complexes between α-(*n*-alkyl) DBKs **2a**−**h** and the capsule formed by **1** are kinetically stable on the NMR time scale, and (b) the guests fall into three packing motifs modulated by the length of the α-alkyl chain. In essence, the host is acting as an external template to promote the formation of distinct guest conformers. We utilize the structures suggested by NMR to understand the variations in photochemical behavior between the eight guests within the capsule.

Following the initial discovery by Turro and co-workers that the product distribution resulting from photolysis of dibenzyl ketone could be controlled by micelles,[22,23] this reaction has become the benchmark to assess the efficacy of a medium as a "cage".[24] The sequence of reactions upon excitation of dibenzyl ketone can be understood on the basis of Scheme 1 (R = H). In solution, as well as in most confined media, the primary radical pair (RP-1) resulting from α-cleavage decarbonylates to yield a secondary aryl methyl radical pair (RP-2).[24] Detailed studies have revealed that the changes in product distribution in organized assemblies are attributable to the restriction on the translational mobility (diffusion) of the primary and secondary radical pairs. Photochemistry of dibenzyl ketones has been investigated in organized assemblies such as micelles, cyclodextrins, and zeolites and in the crystalline state, and a common thread in these processes is the enhanced formation of **3** with respect to **7** and **8** (Scheme 1).[25] Uniquely, in some of these confined media rearrangements, product **9** was obtained in less than 10% yield.[26] Thus, the reaction medium that so greatly influences the coupling of the RP-2 and leads to a large cage effect with essentially only AB products generally has little effect on the reactions of the RP-1 (only a small % of rearranged starting ketone is normally formed). We have recently reported that irradiation of *para*-methyl dibenzyl ketone included within the capsule formed by **1** gave AB (and its rearranged isomers) as the exclusive product of decarbonylation.[10] Most importantly, the rearrangement product **9** from the primary radical pair (Scheme 1) was obtained in significant yield (>50%). Such a remarkable change in product distribution that has not been noted earlier in any other media suggests that this capsule is unique in its ability to influence the behavior of both primary and secondary radical pairs.

To further explore the effectiveness of this capsule as a reaction medium, we have currently examined the photochemistry of α-(*n*-alkyl) dibenzyl ketones (**2a**−**h**) that have multiple chemical channels in the triplet excited-state surface. Ketones **2a**−**h** can cleave on either side of the carbonyl chromophore leading to two rearrangement products (**9** and **10**) and can abstract γ-hydrogen leading to Norrish−Yang products (**11**−**13**). The major products from all eight guests upon irradiation, either in hexane or in buffer solution, resulted from the well-known Norrish type I reaction (Table 2). Independent of the solvent and the alkyl chain, the only products obtained from decarbonylation via Norrish type I process were **3**, **7**, and **8**. No rearrangement products of **3**, namely **4**, **5**, and **6**, and that of the starting ketone, namely **9** and **10**, were formed in any solvent (Scheme 1 and Table 2). The guests that possess γ-hydrogen atoms in the α-alkyl chain gave, via a Norrish type II pathway, products **11**, **12**, and **13** in less than 20% yields. Clearly, in hexane and buffer solutions the Norrish type II process is a minor pathway compared to the type I process. Independent of the fact that both α-cleavage and γ-hydrogen processes were expected to proceed with similar rates, the lower yield of products from the Norrish type II versus Norrish type I could be attributed to the conformational flexibility of the alkyl chain resulting in a lower efficiency of hydrogen abstraction.[27]

Perusal of Table 2 reveals that, relative to either hexane or aqueous solution, the photobehavior of every ketone in the series

(22) (a) Robbins, W. K.; Eastman, R. H. *J. Am. Chem. Soc.* **1970**, *92*, 6076−6079. (b) Engel, P. S. *J. Am. Chem. Soc.* **1970**, *92*, 6074−6075.
(23) (a) Turro, N. J.; Cherry, W. R. *J. Am. Chem. Soc.* **1978**, *100*, 7431−7432. (b) Turro, N. J.; Kraeutler, B. *J. Am. Chem. Soc.* **1978**, *100*, 7432−7434.
(24) (a) Turro, N. J.; Kraeutler, B. *Acc. Chem. Res.* **1980**, *13*, 369−377. (b) Turro, N. J. *Proc. Natl. Acad. Sci. U.S.A.* **1983**, *80*, 609−621. (c) Bhattacharjee, U.; Chesta, C. A.; Weiss, R. G. *Photochem. Photobiol. Sci.* **2004**, *3*, 287−295. (d) Cozens, F. L.; Scaiano, J. C. *J. Am. Chem. Soc.* **1993**, *115*, 5204−5211. (e) Chesta, C. A.; Mohanty, J.; Nau, W. M.; Bhattacharjee, U.; Weiss, R. G. *J. Am. Chem. Soc.* **2007**, *129*, 5012−5022. (f) Kleinman, M. H.; Shevchenko, T.; Bohne, C. *Photochem. Photobiol.* **1998**, *67*, 198−205. (g) Kleinman, M. H.; Shevchenko, T.; Bohne, C. *Photochem. Photobiol.* **1998**, *68*, 710−718.
(25) (a) Quinkert, G.; Tabata, T.; Hickmann, E. A. J.; Dobart, W. *Angew. Chem., Int. Ed. Engl.* **1971**, *10*, 199−200. (b) Veerman, M.; Resendiz, M. J. E.; Garcia-Garibay, M. A. *Org. Lett.* **2006**, *8*, 2615−2617. (c) Resendiz, M. J. E.; Garcia-Garibay, M. A. *Org. Lett.* **2005**, *7*, 371−374. (d) Garcia-Garibay, M. A.; Zhang, Z.; Turro, N. J. *J. Am. Chem. Soc.* **1991**, *113*, 6212−6218. (e) Turro, N. J.; Cheng, C. C.; Abrams, L.; Corbin, D. R. *J. Am. Chem. Soc.* **1987**, *109*, 2449−2456. (f) Gould, I. R.; Zimmt, M. B.; Turro, N. J.; Baretz, B. H.; Lehr, G. F. *J. Am. Chem. Soc.* **1985**, *107*, 4607−4612. (g) Turro, N. J.; Weed, G. C. *J. Am. Chem. Soc.* **1983**, *105*, 1861−1868. (h) Turro, N. J.; Jockusch, S.; Lei, X.-G. *J. Org. Chem.* **2002**, *67*, 5779−5782. (i) Lei, X.-G.; Jockusch, S.; Ottaviani, M. F.; Turro, N. J. *Photochem. Photobiol. Sci.* **2003**, *2*, 1095−1100. (j) Ruzicka, R.; Baráková, L.; Klán, P. *J. Phys. Chem. B* **2005**, *109*, 9346−9353. (k) Petrova, S. S.; Kruppa, A. I.; Leshina, T. V. *Chem. Phys. Lett.* **2004**, *385*, 40−44. (l) Roberts, C. B.; Zhang, J.; Brennecke, J. F.; Chateauneuf, J. E. *J. Phys. Chem.* **1993**, *97*, 5618−5623. (m) Frederick, B.; Johnston, L. J.; de Mayo, P.; Wong, S. K. *Can. J. Chem.* **1984**, *62*, 403−410. (n) Johnston, L. J.; Wong, S. K. *Can. J. Chem.* **1984**, *62*, 1999−2005. (o) Hrovat, D. A.; Liu, J. H.; Turro, N. J.; Weiss, R. G. *J. Am. Chem. Soc.* **1984**, *106*, 5291−5295.
(26) (a) Johnston, L. J.; de Mayo, P.; Wong, S. K. *J. Am. Chem. Soc.* **1982**, *104*, 307−309. (b) Kraeutler, B.; Turro, N. J. *Chem. Phys. Lett.* **1980**, *70*, 266−269. (c) Kraeutler, B.; Turro, N. J. *Chem. Phys. Lett.* **1980**, *70*, 270−275.
(27) (a) Lewis, F. D.; Johnson, R. W.; Johnson, D. E. *J. Am. Chem. Soc.* **1974**, *96*, 6090−6099. (b) Lewis, F. D.; Johnson, R. W.; Kory, D. R. *J. Am. Chem. Soc.* **1974**, *96*, 6100−6107. (c) Wagner, P. J. *Acc. Chem. Res.* **1983**, *16*, 461−467.

2a−**h** has been dramatically altered within the capsule. The first important fact is that the chemical behavior of the secondary radical pair (A, B radical pair, RP-1, Scheme 1) resulting from all eight ketones is uniformly influenced by the capsule. The two radicals A and B resulting via decarbonylation are trapped and forced to combine with or without rearrangement. In all cases, except α-(ethyl) dibenzyl ketone **2b**, no AA or BB was formed within the capsule. Such a large cage effect on the secondary radical pair although noteworthy is not unprecedented in an organized assembly. Similar large cage effect has been noted earlier in micelles, zeolites, and crystals.[24,25] Lack of formation of AA and BB suggests that the capsular assembly is stable in the time scale of the lifetime of the secondary radical pair.[5] The structures of the host−guest complexes shown in Figure 5 account for the presence of cage effect and formation of AB and rearranged AB products.

One of the most interesting features within the capsule is the formation of the rearrangement product(s) of the starting ketone. Such products are formed in less than 10% yield in micelles and zeolites and are not formed in crystals.[25,26] Even more fascinating is that the methyl-, ethyl-, and propyl-substituted dibenzyl ketones yield mostly one rearrangement product (**10**), whereas butyl- and pentyl-substituted dibenzyl ketones give the two rearrangement products **9** and **10**, and hexyl-, heptyl-, and octyl-substituted dibenzyl ketones do not photorearrange. Formation of **10** as the major product from methyl-, ethyl-, and propyl-substituted dibenzyl ketones is consistent with the expectation that the alkyl-substituted α-C−C bond would cleave more readily than the unsubstituted one.[28] Looking at the structures of the complexes presented in Figure 5, it is clear that once the alkyl-substituted α-C−C bond cleaves, the α-substituted benzyl radicals would rotate to optimally fill the cavity and lead to the rearrangement product **10**. Although, in principle, the unsubstituted α-C−C bond could cleave, rotate, and yield **9** as the final product, this probably does not occur because the relative rates of α-cleavage of the substituted and unsubstituted α-C−C bonds favor the former.[28]

As we progress to the butyl- and pentyl-substituted DBKs **2d** and **2e**, the structure of the host−guest complex changes (Figure 5a−e) and, correspondingly, so does the photochemistry. Guests **2a**−**c** pack the capsule such that the two aromatic rings occupy the two hemispheres. Guests **2d** and **2e** pack the capsule such that the hemispheres are filled with the alkyl group and the distal ring. In this packing arrangement, the proximal ring resides at the equatorial region of the capsule. These butyl- and pentyl-substituted dibenzyl ketones yield two rearrangement products **9** and **10** almost in equal amounts. This distinct behavior falls in between shorter chain DBKs (**2a**−**c**) that mainly give one rearrangement product and longer chain DBKs (**2f**−**h**) that give no rearrangement products. Now the question is how the normally slow cleaving unsubstituted α-C−C bond is able to compete with the faster cleaving substituted α-C−C bond. Once again, it is important to recognize that this change in chemistry is specific to the capsule and does not occur in hexane and buffer. We believe that the rates of the α-C−C bond cleavages are not influenced by the capsule, but that the efficiencies of product formation are. In the two structures shown in Figure 5d,e, the "northern" hemisphere is filled with the alkyl chain and accommodation of an aromatic ring following the rearrangement to **10** is expected to be difficult. We believe that templation reduces the efficiency of rotation of the α-alkyl-substituted benzyl radical resulting from **2d** and **2e** forces it to recombine with its partner and regenerate **2d** and **2e**. Such a situation allows the less favored α-cleavage process (unsubstituted α-C−C bond) to compete and yield **9**; rotation of the benzyl radical in the southern hemisphere is readily accomplished, and the packing of the incipient methyl group in the tapering portion of the cavity ensures a driving force toward **9**. Note that in **2d** and **2e** the product **9** is formed at the expense of AB product (Table 2). For example, while in **2c** the ratio of {AB + rearranged AB} to the rearranged ketone is 39:50; in **2d** it is 29:64. However, the data at hand preclude firmly ascertaining the origin of this difference.

Ketones **2f**−**h** do not yield rearrangement products **9** and **10** within the capsule. Structures suggested by ^{1}H NMR provide a clue to this unexpected behavior. In these three cases, the capsule is congested with the guest molecule and there is very little room left for any readjustment of any formed radicals. NMR data reveal that the guests **2f**−**h** pack the cavity of the capsule so that the alkyl group and now the proximal ring fill the two hemispheres, with the distal ring forced to reside in the equatorial region of the host. In this arrangement, the α-substituted benzyl radical would not be able to rotate to yield **10** and there is no driving force for the benzyl radical to rotate. It is interesting to note that the secondary radical pairs stay within the capsule and yield only AB products. Again, this is suggested by the structures shown in Figure 5 where ketones **2f**−**h** are fully accommodated within the capsule and no part of them protrude outside into the external aqueous medium from the slowly assembling and disassembling capsule.

The final point we wish to touch upon relates to the products of Norrish type II reaction. Clearly, in **2h** this becomes the major product (90%). Yields of the Norrish−Yang products are significantly higher in **2f** and **2g** compared to that in **2c**−**e**. Predominance of Norrish−Yang products in **2f**−**h** is consistent with the structures of the host−guest complexes shown in Figure 5. In these structures, the γ-hydrogen is closer to the carbonyl chromophore, a feature that most likely enhances the efficiency of hydrogen abstraction.

Conclusions

The capsule formed by the dimerization of host **1** readily accommodates the α-(*n*-alkyl) DBK guests **2a**−**h**. For the series, however, three different packing motifs are observed. NMR spectroscopy shows that when the R group is small it is the two aromatic rings of the guest that occupy the two hemispheres of the capsule. As the R group increases in length, it displaces the proximal ring from a hemisphere forcing it to reside in the equatorial region of the complex. Ultimately, however, as the R group increases in length further, the proximal ring displaces the distal ring from its hemisphere, forcing the latter to take up residence at the equator. These three packing motifs each lead to distinct photochemical outcomes.

Variation in the photochemistry of the guest within the capsule, with respect to the α-alkyl chain length of the said guest, highlights the importance of how a small variation in

(28) (a) Turro, N. J.; Gould, I. R.; Baretz, B. H. *J. Phys. Chem.* **1983**, *87*, 531−532. (b) Lunazzi, L.; Ingold, K. U.; Scaiano, J. C. *J. Phys. Chem.* **1983**, *87*, 529−530. (c) Tsentalovich, Y. P.; Fischer, H. *J. Chem. Soc., Perkin Trans. 2* **1994**, 729−733. (d) Zhang, X.; Nau, W. M. *J. Phys. Org. Chem.* **2000**, *13*, 634−639.

supramolecular structure can influence the selectivity within a confined nanoscale reactor. It is quite fascinating to be able to control the excited behavior of several α-(alkyl) dibenzyl ketones, all of which behave in an identical manner in solution. It is common knowledge that enzyme active sites can impart specificity on the bound substrate. The results presented here establish that carefully designed synthetic hosts can do likewise, in terms of both their ability to interact with the guest and how templation can influence the reaction course of the guests. The observed selective influence of the capsule formed by cavitand **1** on a variety of guests elucidates specific host designing needs in achieving a specific goal.

Acknowledgment. C.L.D.G. and B.C.G. gratefully acknowledge the National Institutes of Health for financial support (GM074031). V.R. and A.K.S. thank the National Science Foundation for financial support (CHE-0213042 and CHE-0531802).

Supporting Information Available: ^{1}H NMR, ^{13}C NMR, COSY, TOCSY, and NOESY spectra. This material is available free of charge via the Internet at http://pubs.acs.org.

JA7107917